Small-Angle Neutron Scattering Study of Anomalous Mixing Behaviors in Deuterated Polystyrene/Poly(vinyl methyl ether) Mixtures near the Glass Transition Temperature

Hiroyuki Takeno,[†] Satoshi Koizumi,[‡] Hirokazu Hasegawa,[†] and Takeji Hashimoto*[,†]

Department of Polymer Chemistry, Graduate School of Engineering, Kyoto University, Kyoto, 606-01 Japan, and Neutron Scattering Laboratory, Department of Materials Science and Engineering, Japan Atomic Energy Research Institute, Tokai, 319-11 Japan

Received August 21, 1995; Revised Manuscript Received December 21, 1995[⊗]

ABSTRACT: Small-angle neutron scattering (SANS) has been used to investigate the thermal concentration fluctuations in a single-phase state of binary polymer mixtures such as deuterated polystyrene (DPS)/poly(vinyl methyl ether) (PVME), deuterated polybutadiene (DPB)/protonated polybutadiene (HPB), and DPB/protonated polyisoprene (HPI) in a wide range of temperatures from far above the glass transition temperature T_g of mixtures to below the T_g. The DPS/PVME mixture is unique in having a large difference in the T_g's for each pure component compared with the mixtures of DPB/HPB and DPB/HPI having a small difference in the T_g's. The SANS behavior for the DPS/PVME mixture in the single-phase state can be classified into three temperature regimes. At a temperature far above the T_g of the single-phase mixture but below its cloud point, SANS profiles are well described by the scattering formula based upon random phase approximation (RPA) (regime I). As the temperature comes closer to the T_g, the scattering intensity in the low-q region was more suppressed than that expected by RPA (regime II), and the Flory−Huggins interaction parameter was q-dependent. At temperatures below the T_g, the scattering profiles in the entire q region become independent of temperature, frozen due to vitrification (regime III). On the other hand, for both DPB/HPB and DPB/HPI mixtures in the single-phase state, the scattering behaviors can be classified into only two regimes of regime I and regime III. The abnormal scattering behavior observed for regime II seems to be peculiar to the DPS/PVME mixtures with a large difference in the T_g's of pure components.

1. Introduction

The thermal concentration fluctuations (TCF) of polymer mixtures in the single-phase state have been extensively studied from both experimental and theoretical points of view. Small-angle neutron scattering (SANS) made great contributions to the studies of the TCF. There are many indications that the TCF of polymer mixtures in the single-phase state far above their glass transition are described well in the context of incompressible random phase approximation (RPA).[1] The Flory−Huggins interaction parameter χ experimentally determined from the scattering profiles usually has the form as follows.[2,3]

$$\chi = \sigma + h/T \qquad (1)$$

In this work we studied the TCF of polymer mixtures by means of the SANS method down to the temperature range in which the vitrification of the mixtures becomes important. We prepared two types of mixtures, i.e. (i) deuterated polystyrene (DPS)/poly(vinyl methyl ether) (PVME) which has a large difference in the T_g's of the pure components (the T_g's of DPS and PVME are 378 and 251 K, respectively) and (ii) deuterated polybutadiene (DPB)/protonated polybutadiene (HPB) and DPB/protonated polyisoprene (HPI) which have almost equal T_g's for pure components (the T_g's of DPB, HPB, and HPI are 186, 182, and 215 K, respectively). Numerous studies on SANS behaviors in the single-phase state for the DPS/PVME mixture have been made so far.[2,4] However, most of these measurements were carried out at high temperatures at which the systems were free from vitrification. To our knowledge, the anomalous mixing behaviors in the DPS/PVME mixture have not been reported, except for the report by Schwahn et al.[4] on the unusual behavior of the structure factor at scattering vector $q = 0$. For the mixture of DPS/PVME 37/63 vol/vol they carried out SANS measurements down to a temperature of ca. 90 °C, which corresponds to a temperature of ca. 100 K above the T_g of the mixture. Even if measurements are performed near the T_g for particular blends with characteristics which we show in the present paper (see section 4.4), we have to care about the annealing time: the annealing time should be sufficiently long. We emphasize that it is difficult to find the anomalous behavior, unless we pay attention to the annealing time.

Table 1. Sample Characterization

			microstructure, %[c]			
sample	$M_n \times 10^{-3}$ [a]	M_w/M_n[a]	1,2	3,4	cis-1,4	trans-1,4
DPS	102	1.10				
PVME	27[b]	1.40				
DPB	59	1.03	16		38	46
HPB	48	1.20	16		28	56
HPI	78	1.30		7.5	70.4	22.1

[a] Measured by size exclusion chromatography equipped with light scattering. [b] Measured by membrane osmometry. [c] The microstructure for DPB was measured by ^{13}C-NMR, while those for HPB and HPI were measured by IR spectroscopy.

2. Experimental Section

2.1. Sample Preparation and Characterization. The characterization of the polymer samples used in the experiment is summarized in Table 1. DPS, DPB, HPB, and HPI were synthesized by living anionic polymerization. DPB and

* To whom all correspondence should be addressed.
[†] Kyoto University.
[‡] Japan Atomic Energy Research Institute.
[⊗] Abstract published in *Advance ACS Abstracts,* March 1, 1996.

0024-9297/96/2229-2440$12.00/0

Table 2. DSC Results on T_gs for Homopolymer and Blend Samples

neat sample	T_g, K	blend sample	component, wt %/wt %	T_g, K
DPS	378	DPS/PVME	50/50	276
PVME	251	DPS/PVME	70.6/29.4	311
DPB	186	DPB/HPB	49.8/50.2	184
HPB	182	DPB/HPI	59.7/40.3	196
HPI	215			

HPB have almost the same microstructures; i.e., DPB has 38% cis-1,4, 46% trans-1,4, and 16% 1,2 linkages, while HPB has 28% cis-1,4, 56% trans-1,4, and 16% 1,2 linkages. HPB and HPI were kindly supplied by Japan Synthetic Rubber Co. Ltd. PVME was synthesized in toluene by cationic polymerization using boron trifluoride diethyl ether as the initiator. We prepared the binary mixtures of DPS/PVME with the compositions of 50/50 and 70.6/29.4 wt %/wt %. Hereafter we shall designate the composition *X*/*Y* wt %/wt % as *X*/*Y* for simplicity. We also prepared the other binary mixtures of DPB/HPB with the composition of 49.8/50.2 and DPB/HPI with the composition of 59.7/40.3. All the mixtures were dissolved in toluene, and the solvent was evaporated slowly in a Petri dish at room temperature. In order to remove the solvent perfectly, the DPS/PVME films were further dried in a vacuum oven at ca. 80 °C for 2 days. The DPB/HPB and DPB/HPI films were dried at room temperature for 2 days.

2.2. SANS. The small-angle neutron scattering (SANS) experiments were carried out using a 20 m SANS instrument (SANS-J) at the JRR-3M research reactor of the Japan Atomic Energy Research Institute (JAERI) in Tokai. The cold neutrons were monochromatized with a velocity selector to have the wavelength of $\lambda = 6.25$ or 3.57 Å with a distribution of $\Delta\lambda/\lambda = 0.13$, where $\Delta\lambda$ is the full width at half-maximum (fwhm). The scattered neutrons were detected by a two-dimensional Risø-type detector and corrected for empty cell scattering, detector sensitivity, and sample thickness and transmission. The electrical background of this instrument is small enough to be neglected against the observed scattering intensity. The two-dimensional data were circularly averaged to obtain scattering profiles as a function of magnitude of the scattering vector q [$=(4\pi/\lambda)\sin(\theta/2)$ where θ is the scattering angle] and then reduced to absolute units (cm^{-1}) using H_2O as the calibration standard.[5] The coherent scattering intensity was obtained by subtracting the incoherent scattering. For this purpose the incoherent scattering of the blends was estimated from the scattering measurements of the component homopolymers, such as neat PVME for the DPS/PVME and neat HPI for the DPB/HPB and DPB/HPI, because the incoherent scattering of the blend specimens was originated mainly from the hydrogen atoms of the samples. In order to obtain the scattering profiles in a wide q region, the measurements were carried out at the detector position D and with λ as given: ($D = 6$ or 1.5 m, $\lambda = 6.25$ Å) or ($D = 1.5$ m, $\lambda = 3.57$ Å) for the DPS/PVME 50/50; ($D = 6$ or 1.5 m, $\lambda = 6.25$ Å) for the DPS/PVME 70.6/29.4; ($D = 10$ or 1.5 m, $\lambda = 6.38$ Å) for the DPB/HPB; ($D = 10$ m, $\lambda = 6.85$ Å) for the DPB/HPI.

2.3. DSC. T_g's of the homopolymers and the polymer mixtures were measured using Perkin-Elmer DSC apparatuses (DSC-7 and DSC-2C). The DSC measurements were performed in the heating cycle with the heating rate of 20 K/min in the temperature range 228−398 K for the DPS/PVME mixtures, 228−448 K for neat DPS, 180−286 K for neat PVME, and 145−271 K for DPB/HPB and DPB/HPI mixtures as well as for neat DPB, HPB, and HPI. The calibration of the DSC-7 was performed according to the heat of fusion of indium and *n*-octadecane standards and that of the DSC-2C was performed by the heat of fusion of *n*-octane and *n*-dodecane standards. T_g was determined as the midpoint of the endothermic DSC curve observed.

3. Experimental Results

3.1. DSC. The T_g's of the binary mixtures and the neat component polymers determined by DSC are summarized in Table 2. A single T_g was observed for all the mixtures, suggesting that they are in the single-phase states. According to the results, it should be stressed that the mixtures of DPB/HPB and DPB/HPI have a small difference in the T_g's which are 4 and 29 K, respectively. On the other hand, the mixture of DPS/PVME has a large difference in the T_g's which is 127 K.

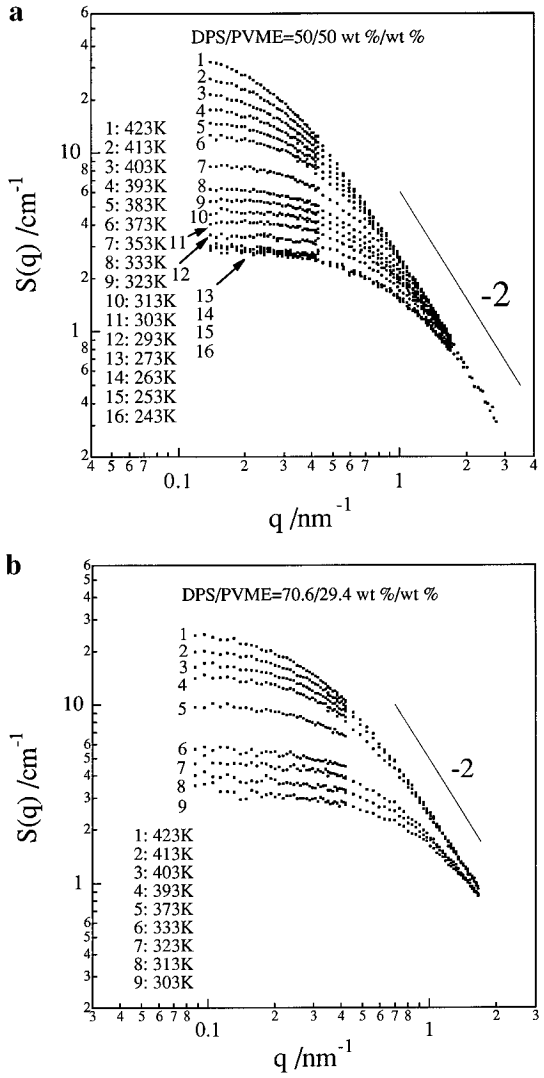

Figure 1. SANS profiles for the DPS/PVME (a) 50/50 and (b) 70.6/29.4 mixtures at various temperatures.

3.2. SANS. As is well-known, the mobility of polymers becomes very small near their T_g. Therefore, it is important to specify the thermal programs in our SANS measurements near T_g. We carried out the SANS measurements for all the mixtures in cooling cycles from far above the T_g down to near the T_g of the mixtures. All the measurements were started after the system was equilibrated at the specified temperatures for ca. 25−30 min.

Figure 1 shows the double logarithmic plots of the SANS profiles for the mixtures of DPS/PVME 50/50 (a) and 70.6/29.4 (b) at various temperatures. The temperature range of the measurement was 243−423 K for DPS/PVME 50/50 and 303−423 K for DPS/PVME 70.6/29.4. The T_g's for the two mixtures were determined to be 276 and 311 K from the DSC measurements, respectively. Thus the temperature range for SANS measurements extends from far above the T_g's of the mixtures to below them. The q range of SANS measurements is 0.139−2.72 nm^{-1} for the DPS/PVME 50/

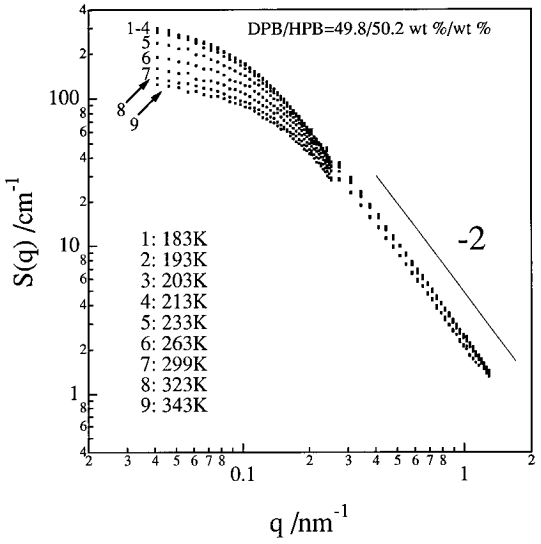

Figure 2. SANS profiles for the DPB/HPB mixture at various temperatures.

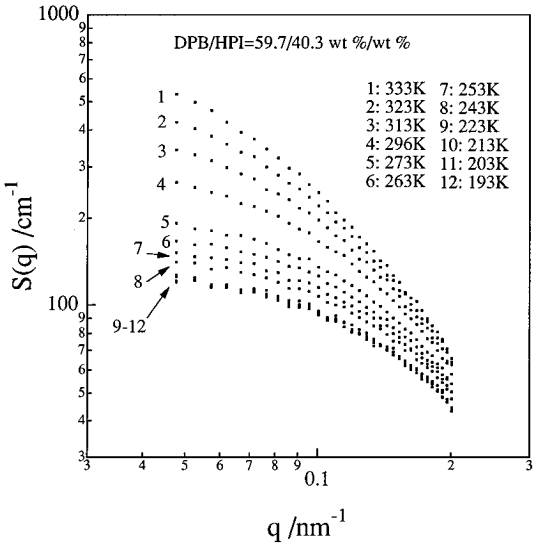

Figure 3. SANS profiles for the DPB/HPI mixture at various temperatures.

50 mixture and 0.087−1.66 or 0.418 nm^{-1} for the DPS/PVME 70.6/29.4 mixture. At each temperature, the scattering profiles for both mixtures show the monotonous decreases of the scattering intensity as a function of q, showing the asymptotic behavior of q^{-2} in the high-q region. As the temperature increases, the scattering intensity for both mixtures increases in the low-q region, which indicates that DPS/PVME has a phase diagram with the LCST behavior. In other words, the TCF becomes larger as the temperature is raised close to the phase boundary. In the temperature region below 273 K, which is expected to be the T_g of the mixture, the scattering profiles for the DPS/PVME 50/50 mixture shows no change with temperature in the entire q region observed. TCF is frozen, because the mobility of polymers is extremely low below the T_g. Therefore, it is expected that the relaxation time of TCF becomes longer than the time scale of the measurements.

Figure 2 shows the double logarithmic plot of the SANS profiles obtained for the DPB/HPB mixture in the temperature range of 183−343 K. It should be mentioned that the T_g of the mixture obtained by DSC was 184 K, which is close to the lowest limit of our SANS measurements. The q range of the measurement was 0.04−1.29 nm^{-1}. At each temperature, the scattering profiles show the monotonous decreases in the scattering intensity as a function of q, showing the asymptotic behavior of q^{-2} in the high-q region. In the low-q region, the scattering intensity increases with decreasing temperature, indicating that the DPB/HPB mixture has a phase diagram with an upper critical solution temperature (UCST) behavior. In the temperature region below 193 K, the scattering profiles become independent of temperature in the entire q range observed, probably due to vitrification of the mixture. This temperature (193 K) is slightly higher than the T_g (184 K) determined by DSC measurement.

Figure 3 shows the double logarithmic plot of the SANS profiles for the DPB/HPI mixture in the temperature range 193−333 K. It should be stressed that the T_g for this mixture obtained by DSC was 196 K, which is the lowest bound of the temperature range in our SANS measurements. The q range for SANS is 0.0477−0.200 nm^{-1}. The scattering profiles for DPB/HPI show the monotonous decreases of the scattering intensity as a function of q. In this case the q range of the SANS data was not enough to observe the asymptotic behavior of q^{-2} in the high-q region. In the low-q region the scattering intensity increases with increasing temperature, which means that the DPB/HPI mixture[3] has an LCST-type phase diagram, as is the case of the DPS/PVME mixtures.[2]

4. Analysis and Discussion

4.1. Conventional Mean-Field Theory Based on RPA. de Gennes presented the static structure factor $S(q)$ for a binary mixture in the single-phase state on the basis of RPA.[1] So far the structure factor $S(q)$ for the polymer mixtures, in which the condition of incompressibility is ensured, is well described by the de Gennes theory. For the mixtures of component polymers 1 and 2 having asymmetric segmental volume and the polydispersity in the molecular weight given by the Schultz−Zimm distribution, $S(q)$ is modified as follows:[6]

$$\frac{k_N}{S(q)} = \frac{1}{\phi_1 N_{n,1} v_1 g_D(x_1)} + \frac{1}{\phi_2 N_{n,2} v_2 g_D(x_2)} - \frac{2\chi}{v_0} \quad (2)$$

with

$$k_N = N_0\left(\frac{a_1}{v_1} - \frac{a_2}{v_2}\right)^2 \quad (3)$$

and

$$g_D(x_i) = \left[x_i - 1 + \left(\frac{h_i}{h_i + x_i}\right)^{h_i}\right] \quad (4)$$

where

$$x_i = q^2 R_{g,i}{}^2 = \frac{q^2 N_{n,i}{}^2 b_i{}^2}{6} \quad (5)$$

and

$$h_i = \left\{\left(\frac{N_w}{N_n}\right)_i - 1\right\}^{-1} \qquad (i = 1 \text{ or } 2) \quad (6)$$

Here $N_{n,i}$ and $N_{w,i}$ denote the number- and weight-average degree of polymerization for the ith component (i = 1 or 2). ϕ_i is the volume fraction for component i

with the volume of the monomeric unit v_i, the mean square radius of gyration of molecule $R_{g,i}$, and statistical segment length b_i, a_i is the neutron scattering length of the monomeric unit for component i. N_0 is Avogadro's number, and v_0 is the molar volume of the reference cell calculated by $v_0 = (\phi_1/v_1 + \phi_2/v_2)^{-1}$. $g_D(x_i)$ is the well-known Debye function for an isolated Gaussian chain of component i. χ denotes the Flory segmental interaction parameter.

For small q values, the expansion of eq 2 in powers of q up to q^2 leads to an expression in Ornstein−Zernike (O−Z) form, as follows:

$$S^{-1}(q) = S^{-1}(0)[1 + q^2\xi^2] = S^{-1}(0) + Aq^2 \qquad (7)$$

$S(0)^{-1}$ is related to the free energy of mixing per unit volume Δg_m.

$$S^{-1}(0) = \frac{1}{k_N}\partial^2\left(\frac{\Delta g_m}{RT}\right)/\partial\phi^2 = \frac{1}{k_N}\left(\frac{1}{\phi_1 N_{w,1} v_1} + \frac{1}{\phi_2 N_{w,2} v_2} - \frac{2\chi}{v_0}\right) \qquad (8)$$

and

$$A = \frac{1}{3k_N}\left[\frac{J_1 {R_{g,1}}^2}{\phi_1 N_{w,1} v_1} + \frac{J_2 {R_{g,2}}^2}{\phi_2 N_{w,2} v_2}\right] \qquad (9)$$

with

$$J_i = \left\{2\left(\frac{N_{w,i}}{N_{n,i}}\right) - 1\right\} \qquad (10)$$

Furthermore, the correlation length ξ for the TCF is given by

$$\xi^2 = AS(0) \qquad (11)$$

4.2. SANS Profiles in the Low-*q* Region. In this section, we will discuss the temperature dependence of SANS profiles in the low-q region. Figure 4 shows the O−Z plots [$S(q)^{-1}$ vs q^2 plot] for the DPS/PVME mixtures with the compositions of (a) 50/50 and (b) 70.6/29.4 at various temperatures. Figures 5 and 6 also show the O−Z plots for DPB/HPB and DPB/HPI, respectively. As shown in Figures 4−6, the reciprocal values of $S(q)$ in low-q regions are well fitted with a linear function of q^2. The slope of the O−Z plot for the DPS/PVME 50/50 mixture gradually decreases as the temperature gets close to the T_g (276 K). However, at a temperature (283 K) just above the T_g, the slope suddenly increases. On the other hand, the slopes of the O−Z plots for the other blends show almost no change with the temperatures. These behaviors will be more clearly shown in Figures 10 and 11, discussed in detail later. The value of $S(0)^{-1}$, which is obtained from the linear extrapolation of the O−Z plot to $q = 0$, is related to the thermodynamic stability of a given mixture, e.g. $S(0)^{-1}$ becomes zero at the spinodal point of the mixture.

Figure 7 shows the temperature dependence of $S(0)^{-1}$ thus obtained as a function of reciprocal absolute temperature T^{-1} for the DPS/PVME (a) 50/50 and (b) 70.6/29.4 mixtures. The error bars are smaller than the size of data symbols in this figure, so that the error bars are not attached especially to the data points. Similarly, in the following figures we omit error bars in the case of error smaller than the size of data symbols. In Figure 7, we can find three regimes (I−III) for the DPS/PVME 50/50 mixture and two regimes (I and II) for the DPS/PVME 70.6/29.4 mixture as a function of T^{-1}. Regime III for the latter should be observed if the experiments

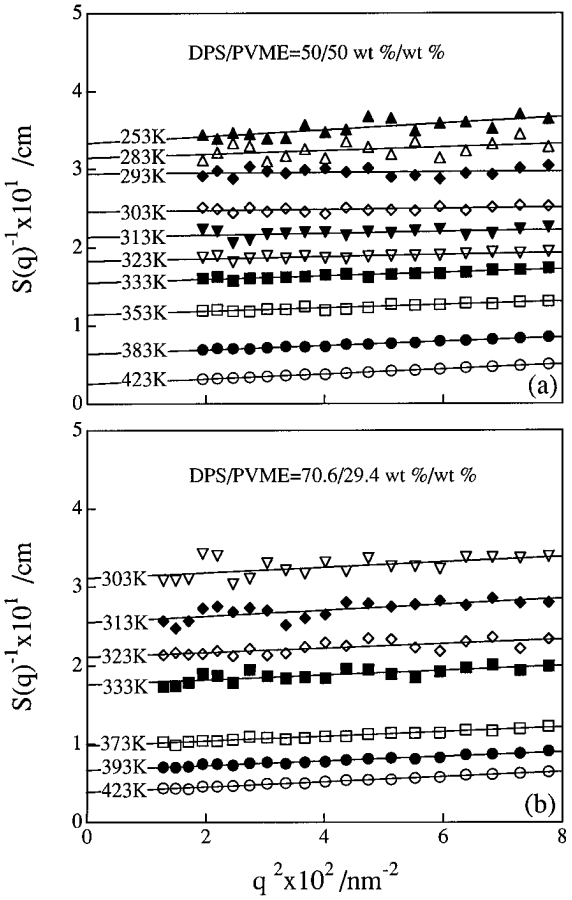

Figure 4. Plots of $S(q)^{-1}$ against the square of the scattering vector q for the DPS/PVME (a) 50/50 and (b) 70.6/29.4 mixtures at various temperatures.

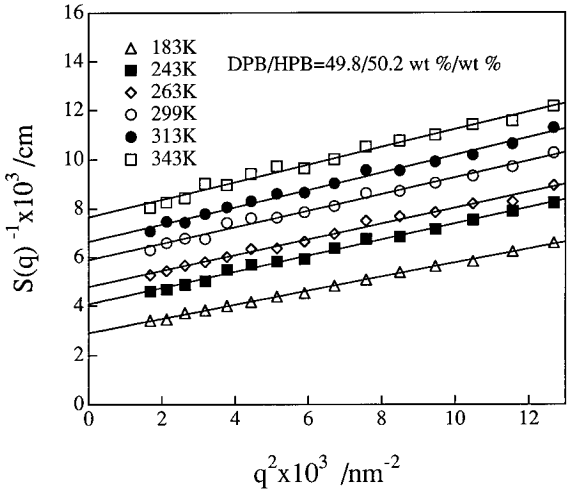

Figure 5. Plots of $S(q)^{-1}$ against the square of the scattering vector q for the DPB/HPB mixture at various temperatures.

were conducted to much lower temperatures. Regime I is in the temperature region much higher than the T_g of the mixture. So far most of the SANS studies on TCF in polymer mixtures have been carried out in this regime which is free from vitrification. In this regime, $S(0)^{-1}$ increases linearly with T^{-1} so that we find

$$S(0)^{-1} = -0.339 + 154/T \qquad (12)$$

and

$$S(0)^{-1} = -0.331 + 156/T \qquad (13)$$

for the DPS/PVME 50/50 and 70.6/29.4 mixtures, re-

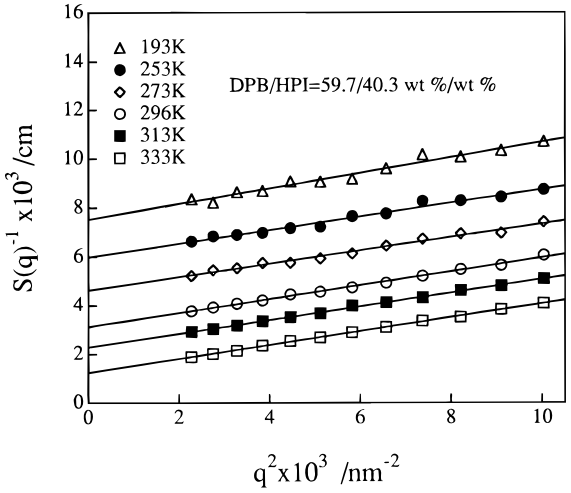

Figure 6. Plots of $S(q)^{-1}$ against the square of the scattering vector q for the DPB/HPI mixture at various temperatures.

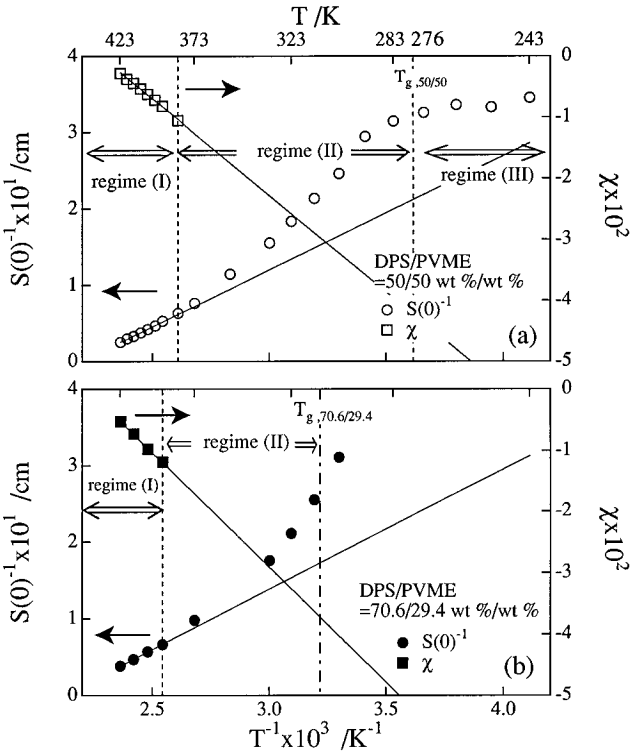

Figure 7. Plots of reciprocal zero wavenumber structure factor $S(0)^{-1}$ and Flory−Huggins parameter χ vs inverse temperature for the DPS/PVME (a) 50/50 and (b) 70.6/29.4 mixtures.

spectively. Here the mean-field spinodal temperatures T_s, at which $S(0)^{-1} = 0$ can be determined, are 454 and 471 K for the 50/50 and 70.6/29.4 mixtures, respectively.

The temperature ranges of 383−273 and 393−303 K for the DPS/PVME 50/50 and 70.6/29.4 mixtures, respectively, correspond to regime II. In this regime, $S(0)^{-1}$ deviates from the temperature dependence obtained in regime I: $S(0)^{-1}$ increases more rapidly with T^{-1} in regime II than in regime I. Deviation of $S(0)^{-1}$ from the linear dependencies on T^{-1} takes place at 383 and 393 K for the 50/50 and 70.6/29.4 mixtures, respectively. This deviation becomes larger as the temperature becomes closer to T_g. These phenomena have been reported by Schwahn et al. for a DPS/PVME mixture.[4] We should note that the DPS/PVME mixtures have a large difference in the T_g's of the pure components. This unexpected increase in $S(0)^{-1}$, or the unexpected suppression of $S(0)$ suggests that osmotic compressibility of the mixture tends to be suppressed more strongly than the suppression predicted by the incompressible RPA theory, with decreasing temperature closer to the T_g of the mixture.

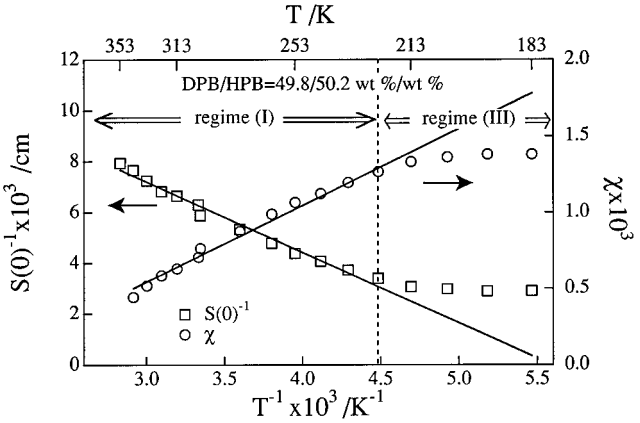

Figure 8. Plots of reciprocal zero wavenumber structure factor $S(0)^{-1}$ and Flory−Huggins parameter χ vs inverse temperature for the DPB/HPB mixture.

Regime III corresponds to the temperature range 273−243 K for the DPS/PVME 50/50 mixture. In this regime, $S(0)^{-1}$ does not change with T^{-1}. This implies that the TCF in the mixtures was frozen due to the vitrification. Thus we can determine the freezing temperature of the TCF which is very close to the T_g determined by DSC. However, it should be noted that the freezing temperature may be strongly influenced by the experimental conditions such as the cooling rate, because of the nonequilibrium effect remaining in the mixtures.

We emphasize that the unexpected phenomenon observed in regime II for the DPS/PVME mixture is not due to the nonequilibrium effect. The SANS measurements were carried out by the cooling process as mentioned in section 3.2. If the system had been trapped in the nonequilibrium state at a given temperature near T_g, $S(0)^{-1}$ should have been smaller than that expected from RPA; i.e., $S(0)^{-1}$ vs T^{-1} plots should have deviated downward from the straight line. However, in regime II, $S(0)^{-1}$ vs T^{-1} plots for both DPS/PVME mixtures deviated upward.

On the other hand, completely different temperature dependencies of $S(0)^{-1}$ were observed for the DPB/HPB and DPB/HPI, as shown in Figures 8 and 9. The temperature dependencies of $S(0)^{-1}$ for both mixtures are classified into two regimes corresponding to regimes I and III defined for the DPS/PVME mixtures. In regime I above T_g (223−343 and 243−333 K for the DPB/HPB and DPB/HPI mixtures, respectively), $S(0)^{-1}$ changes linearly with T^{-1}. Upon decreasing temperature, the temperature dependence of $S(0)^{-1}$ changes from regime I to III without going through regime II. In the temperature ranges of 193−223 and 213−243 K, respectively, for the mixtures of DPB/HPB and DPB/HPI, which are believed to be just above their T_g's, $S(0)^{-1}$ shows only the gradual change with T^{-1}. This behavior implies that as the temperature approaches the T_g of the mixture, the dynamics toward the equilibrium state becomes slower and the mixtures are trapped in a nonequilibrium state. At temperatures below 193 and 213 K for the mixtures of DPB/HPB and DPB/HPI, respectively, $S(0)^{-1}$ becomes constant, due to the vitrification. Here it should be denoted that the T_g

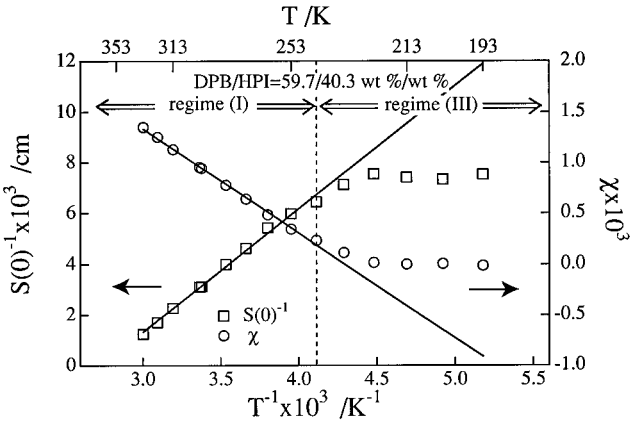

Figure 9. Plots of reciprocal zero wavenumber structure factor $S(0)^{-1}$ and Flory−Huggins parameter χ vs inverse temperature for the DPB/HPI mixture.

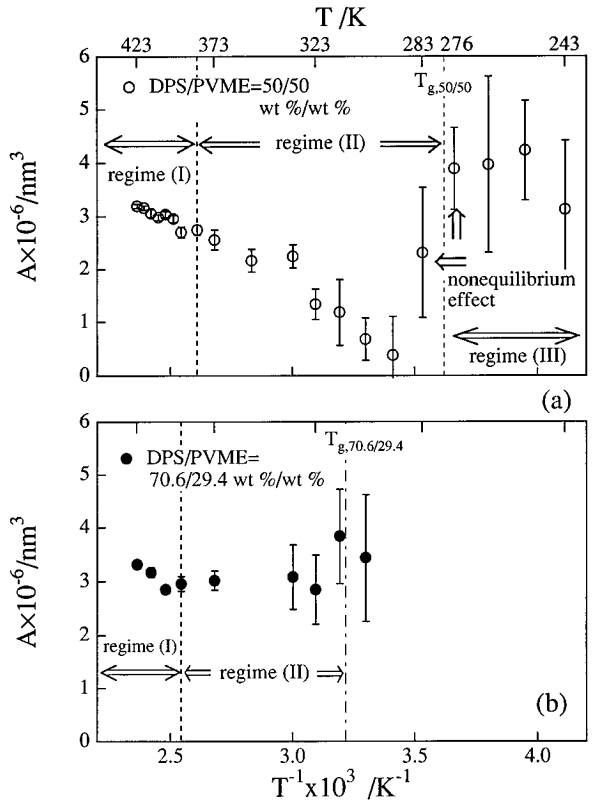

Figure 10. Slope of Ornstein−Zernike plot as a function of reciprocal temperature for the DPS/PVME (a) 50/50 and (b) 70.6/29.4 mixtures.

thus evaulated by SANS is slightly higher than that determined by the DSC measurements. This discrepancy again reflects the difference in the temperature programs used in these two experiments. The program for the SANS experiment took a much longer time than that for the DSC experiment.

Thus the scattering behavior of regime II is unique to the DPS/PVME mixtures which have a large difference in the T_g's of the pure components, while this regime was not observed for the mixtures of DPB/HPB or DPB/HPI, which has the small difference in the T_g's of the pure components.

It is noteworthy to estimate the temperature dependence of the slope A in the O−Z plot. If the parameters R_g and v_i in eq 9 do not have any temperature dependence, A should be independent of T from the prediction of the conventional RPA equation (see eq 9). Figure 10

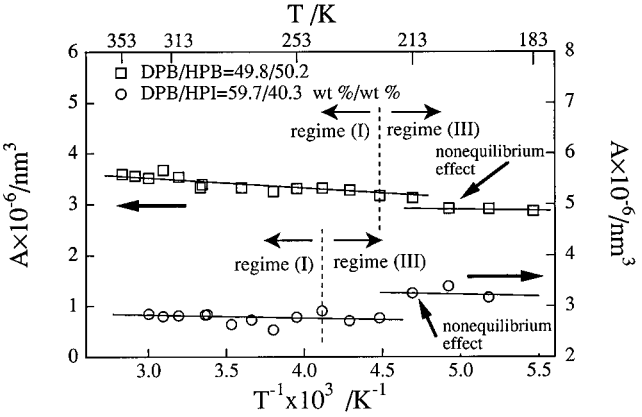

Figure 11. Slope of Ornstein−Zernike plot as a function of reciprocal temperature for the DPB/HPB (square) and DPB/HPI (circle) mixtures.

shows the plots of A as a function of T^{-1} for the DPS/PVME (a) 50/50 and (b) 70.6/29.4 mixtures. In the temperature range corresponding to regime I, A shows only a little change for both mixtures. However, in regime II, A decreases markedly for the DPS/PVME 50/50 mixture. It should be stressed that the degree of this decrease is much larger than that expected from the thermal expansions of R_g and v_i; e.g. the thermal expansivity of the unperturbed chain dimension for PS is given by $[\mathrm{d} \ln(R_g^2)/\mathrm{d}T = -1.1 \times 10^{-3}\ \mathrm{K}^{-1}]$[7] and the thermal expansion coefficient $1/V(\partial V/\partial T)$ for PS is $(5.1-6.0) \times 10^{-4}\ \mathrm{K}^{-1}$].[8] The unexpected change of A will be shown to be explained by taking into account the q dependence of the χ parameter, in the context of the incompressible RPA (see section 4.4 for the details).

At a temperature between 283 and 298 K, the value of A for the 50/50 mixture jumps up as shown in Figure 10a. This phenomenon will be discussed in section 4.5. At temperatures below 273 K, A becomes constant due to the vitrification of the mixture. On the other hand, for the 70.6/29.4 mixture the decrease of A was not as significant as that for the 50/50 mixture. We speculate that this result for the 70.6/29.4 mixture was due to insufficient annealing time. As is mentioned in section 1, we stress that the anomalous behavior near the T_g is strongly affected by annealing time. Hence, in order to perfectly understand the behavior, we must have enough information concerning dynamics of the systems under consideration, e.g. the relaxation time of TCF. The study of composition dependence of the relaxation process of TCF will be the subject of future work.

Figure 11 shows the changes in A as a function of T for the mixtures of DPB/HPB and DPB/HPI. In contrast with the DPS/PVME mixtures, A is independent of T in both regimes I and III, as described by eq 9. Thus the unexpected behaviors for the DPS/PVME mixture in regime II seem to be related to the large difference in the T_g's of the pure components. Studies for other blends with very different T_g's will be carried out in future work.

4.3. SANS Profile in the Whole *q* Region. In this section, we discuss the SANS profiles in the whole q region covered in this experiment. Flory's interaction parameter χ was estimated by curve-fitting of eq 2 to the SANS profiles in regime I, in which the vitrification is not important. Parts a and b of Figure 7 show the estimated χ for the DPS/PVME 50/50 and 70.6/29.4 mixtures, respectively, as a function of T. The temperature dependencies of χ for both mixtures show a good

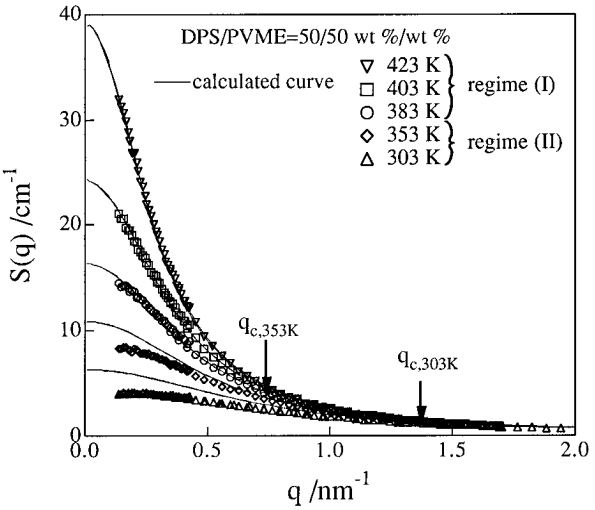

Figure 12. Comparison of experimental SANS profiles with the theoretical curves (solid line) calculated by using eqs 2 and 14a for the DPS/PVME 50/50 mixture.

linearity with T^{-1} in regime I and are described by

$$\chi = 0.0702 - 30.9/T \quad \text{(for DPS/PVME 50/50)} \tag{14a}$$

$$\chi = 0.0817 - 36.8/T \quad \text{(for DPS/PVME 70.6/29.4)} \tag{14b}$$

We calculated the scattering functions at the temperatures corresponding to regimes I and II by using eq 2 and eq 14a for the temperature dependence of χ. Figure 12 shows the scattering functions thus estimated and the SANS profiles for the DPS/PVME 50/50 mixture. At the temperatures corresponding to regime I, e.g. 383, 403, and 423 K, the calculated scattering function (solid lines) shows a good agreement with the experimental profiles (symbols), whereas at the temperatures in regime II, e.g. 303 and 353 K, the calculated function (solid lines) deviates upward from the experimental one especially in the low-q region. Nevertheless, even in regime II, there is a nice agreement between the experimental profiles and the calculated scattering functions in the higher q region.

Figure 13 shows the differences between the theoretical $[S(q)_{\text{theory}}]$ and experimental structure factors $[S(q)]$ normalized by $S(q)$, for the DPS/PVME 50/50 mixture at various temperatures. The degree of deviations in the low-q region becomes larger as the temperature becomes closer to the T_g of the mixture (276 K). The result indicates that near the T_g the intensities of the long wavelength modes of TCF tend to be suppressed compared with those expected by the incompressible RPA theory. In addition, the critical wavenumber q_c, below which the deviation becomes significant, can be determined at each temperature. It shifts toward a higher q as the temperature approaches the T_g, as shown in Figure 14. The q region in which TCF is suppressed becomes wider as the temperature approaches the T_g.

By using eq 2, χ was also estimated for the mixtures of DPB/HPB and DPB/HPI in regime I and regime III (see Figures 8 and 9). The obtained χ values also show the good linearity with T^{-1} in regime I. On the other hand, χ remains constant in regime III where the TCF is frozen due to vitrification.

4.4. Modified RPA Theory. As we mentioned in sections 4.2 and 4.3, the SANS behavior for the DPS/PVME 50/50 mixture in regime II, i.e., the suppression of $S(q)$ at $q < q_c$, and the remarkable decrease of A near the T_g cannot be explained by the conventional RPA theory. Recently, several theoretical attempts which take into account the compressibility effects on scattering function have been made.[9−13] Therefore, it may be expected that our anomalous behaviors of $S(q)$ at $q < q_c$, and A in regime II have been caused by such compressible effects. However, it has been recently shown in Bidkar and Sanchez that the apparent radius of gyration, or statistical segment length, is overestimated, if we analyze the scattering data predicted from the compressible polymer blends by using the conventional RPA theory.[9] If our scattering data in the low-q region are analyzed by using the conventional RPA, then the value of the statistical segment length obtained

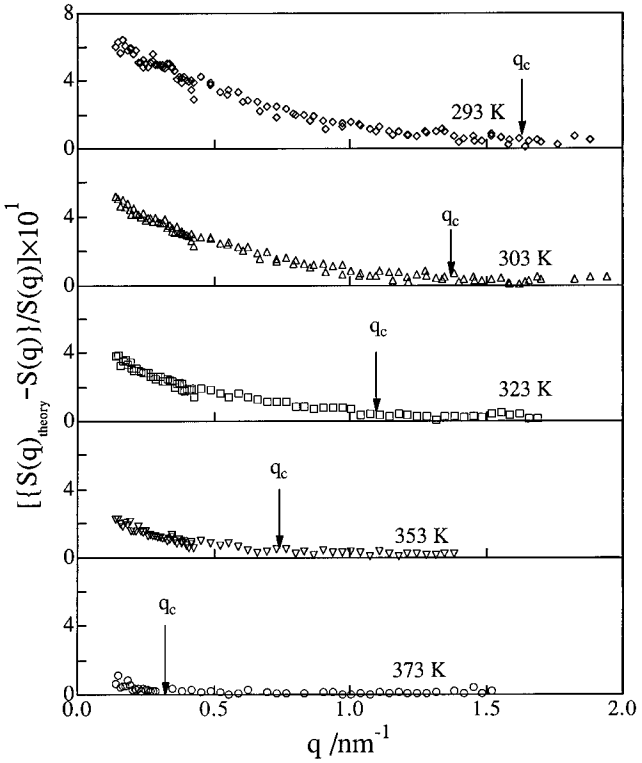

Figure 13. Plots of the differences between the theoretical curves, $S(q)_{\text{theory}}$, and the experimental structure factors, $S(q)$, which are normalized by $S(q)$, as a function of q at various temperatures. The arrow shows the position of q_c at each temperature.

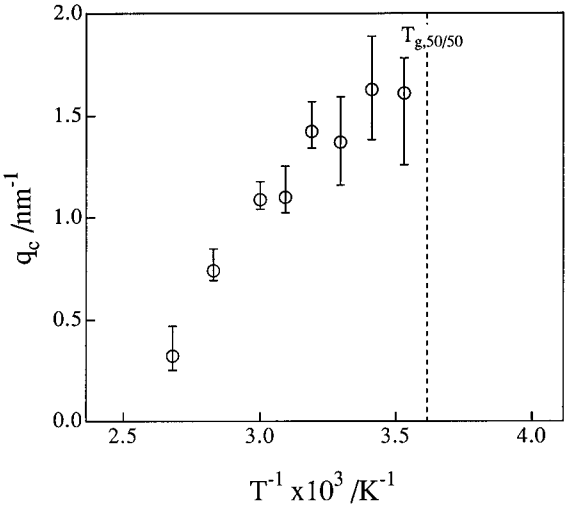

Figure 14. Plots of q_c as a function of reciprocal temperature.

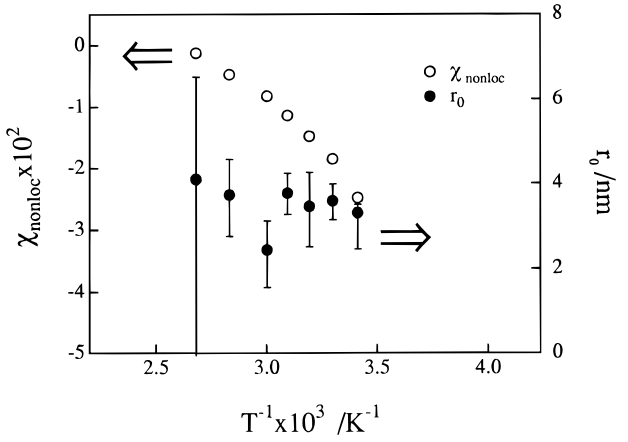

Figure 15. Plots of χ_{nonloc} and r_0 against reciprocal temperature.

becomes 2.3 Å at $T = 293$ K. It is too small. Moreover, according to Bidkar and Sanchez, this value should be *overestimated* rather than underestimated. Hence, we tentatively interpret that the anomalous behaviors we found may not be due to the compressible effects.

Here, we analyze the anomalous SANS behavior in regime II, in the context of the incompressible RPA, by taking the q dependence of χ into account.[14,15]

$$\chi(q) = \chi_{loc} + \chi_{nonloc}\left(1 - \frac{r_0^2 q^2}{6}\right) + O(q^4) \qquad (15)$$

χ_{loc} denotes local contributions of the effective χ parameter which originate from the local interaction of the segments. χ_{nonloc} denotes nonlocal contributions of the effective χ parameter which affect the q dependence of χ. r_0 is the interaction range parameter. Using eq 15, $S(0)^{-1}$ and A are modified as follows.

$$\frac{1}{S(0)} = \frac{1}{k_N}\left(\frac{1}{\phi_1 N_{w,1} v_1} + \frac{1}{\phi_2 N_{w,2} v_2} - \frac{2}{v_0}(\chi_{loc} + \chi_{nonloc})\right) \qquad (16)$$

and

$$A = \frac{1}{3k_N}\left[\left(\frac{J_1 R_{g,1}^2}{\phi_1 N_{w,1} v_1}\right) + \left(\frac{J_2 R_{g,2}^2}{\phi_2 N_{w,2} v_2}\right) + \frac{\chi_{nonloc} r_0^2}{v_0}\right] \qquad (17)$$

Here, we assume that the contribution of χ_{nonloc} is significant only in regime II and small enough to be neglected in regime I. Therefore, χ_{loc} is expressed by eq 14a

$$\chi_{loc} = 0.0702 - 30.9/T \qquad (18)$$

for the DPS/PVME 50/50 mixture. Using eq 18, we can estimate χ_{nonloc} from the values of $S(0)^{-1}$ in regime II. In addition, r_0 can be estimated from the values of slope A and χ_{nonloc} by using eq 17. The results obtained are shown in Figure 15. As shown in Figure 15, χ_{nonloc} is negative and the absolute value becomes larger, as the temperature becomes closer to the T_g. The result indicates that the nonlocal term of the attractive interactions (χ_{nonloc}) and the well-known local attractive interaction term (χ_{loc}) increase upon approaching T_g. This nonlocal term is responsible for suppressing the amplitude of TCF with long wavelengths. On the other hand, the value of r_0 obtained is ca. 3−4 nm independent of the temperature.

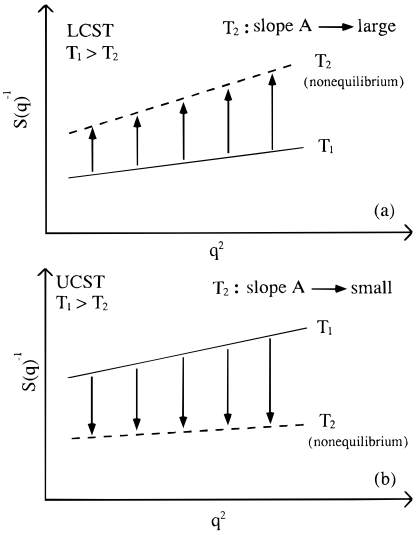

Figure 16. Schematic representation of the nonequilibrium effect on the Ornstein−Zernike plot for system with (a) LCST and (b) UCST type of phase behavior.

Recently, Khokhlov et al. theoretically predicted that for the polymer blends with a large difference in the T_g's of the pure components, the effective χ parameter has the q dependence and that the scattering function at small q is suppressed relative to that predicted by the conventional RPA theory near the T_g of the mixture.[15] According to them, it is expected that such suppression of scattering intensity at low q will be observed for polymer blends which have the following characteristics:[15] (i) two components have very different T_g's and (ii) at least one component has a bulky side group, so that their rotations are increasingly intercorrelated in space upon lowering the temperature toward the T_g of the blend in the single-phase state. In such blends the rotational entropy makes a negative contribution to the χ parameter and the nonlocality of the rotational entropy is expected to become increasingly significant upon lowering the temperature toward the T_g. The entropy causes a decrease in the free energy of low-q modes of the system. That is, the entropy leads to the suppression of TCF with long wavelengths. In addition, they suggest that under a given condition "microphase separation" for the mixture may take place near the T_g, which strongly suppresses the scattering intensity near $q \to 0$ as in the case of block copolymers, resulting in the scattering profile with a maximum.

In this work, though "microphase separation" or a maximum in the scattering profile was not observed, the anomalous SANS behavior in regime II, namely the suppression of the scattering intensity in the low-q region, shows a good qualitative agreement with their theory.

4.5. Nonequilibrium Effect. For our SANS experiments, we annealed sample specimens for ca. 25−30 min at each temperature. As the temperature becomes closer to the T_g, the mobility of polymer chains becomes very low so that the time required for equilibration becomes longer. If the annealing time is not long enough, the mixture cannot attain the equilibrium state. For the DPS/PVME 50/50 mixture, the slope A for the O−Z plot suddenly increased at the temperature close to the T_g (see Figure 10a). We believe that this phenomenon is due to a nonequilibrium effect, i.e. the q dependence in the relaxation time of the TCF. In

general, the relaxation time of the TCF is faster for the Fourier modes having a higher wavenumber q. As shown in Figure 16a, if measurement is carried out by changing the temperature from T_1 to T_2 ($T_1 > T_2$), then the TCF decreases for the system which has an LCST-type phase behavior; i.e. $S(q)^{-1}$ increases. Taking into consideration the q dependence of the relaxation time of the TCF, in the nonequilibrium state, the value of $S(q)^{-1}$ in the high-q range increases with time at a larger rate. Therefore, the slope A becomes bigger than that of the equilibrium state. On the other hand, the nonequilibrium effect for the system with a UCST-type phase behavior is opposite. The TCF increases by changing the temperature from T_1 to T_2 ($T_1 > T_2$); i.e. $S(q)^{-1}$ decreases. As the values $S(q)^{-1}$ in the high-q range decrease at a larger rate, the slope A becomes smaller than that of the equilibrium state (Figure 16b).

The nonequilibrium effect is also observed for the DPB/HPB and DPB/HPI mixtures if we observe Figure 11 carefully. The A value for the DPB/HPI mixture suddenly increased at 213 K, while that for the DPB/HPB mixture decreased slightly at 203 K.

5. Conclusion

By using SANS techniques, we studied the thermal concentration fluctuations for two types of polymer mixtures, i.e. (i) DPS/PVME mixtures having a large difference in the T_g's of the pure components and (ii) mixtures of DPB/HPB and DPB/HPI having a small difference in T_g's of pure components. The range of temperature covered is very wide, from far above T_g to below the T_g of the mixture. We found that as the temperature comes closer to T_g, the scattering profiles $S(q)$ for the mixtures of DPS/PVME showed a significant deviation from the scattering function obtained in the context of incompressible RPA. In other words, the scattering intensity in the low-q region is suppressed relative to that predicted by the conventional RPA theory; the degree of suppression tends to increase with decreasing q. The suppression is more significant as the temperature approaches the T_g. To our surprise, the deviation took place from the temperature ca. 107 K above the T_g for the DPS/PVME 50/50 mixture. Furthermore, our SANS data suggest that in this temperature regime the effective interaction parameter shows the q dependence of the type given by eq 15. On the other hand, the SANS behavior for both blends of DPB/HPB and DPB/HPI was well described by the conventional de Gennes scattering formula at all the temperatures.

It is expected from our SANS results that the deviation from de Gennes' scattering formula near the T_g was caused by the following characteristics of the DPS/PVME mixture: (i) the DPS/PVME mixture has very different T_g's in pure components and (ii) DPS has a bulky side group, i.e., bulky benzene ring, while PVME does not have any bulky side groups. Hence, it is predicted that the rotational entropy made a significant contribution to attractive interaction term and the nonlocality of the rotational entropy became increasingly important upon approaching the T_g of the mixture.

Acknowledgment. We are grateful to Prof. A. R. Khokhlov for very useful discussions which motivated the present study. We thank Mr. Izuka and Mr. Sumimoto at the Daicel Co., Ltd., Japan, for helping with DSC measurements. We gratefully acknowledge Dr. J. Suzuki and Mr. Shimojyo at the Japan Atomic Energy Research Institute, Japan, for helping with SANS measurements. A part of this work was supported by a Grant-in-Aid for Scientific Research in Priority Areas "Cooperative Phenomena in Complex Fluids" (07236103) from the Ministry of Education, Science, and Culture, Japan, and also by scientific grants from Japan Synthetic Rubber Co., Ltd., Japan, and from NIPPON ZEON Co., Ltd.

References and Notes

(1) de Gennes, P.-G. *Scaling Concepts in Polymer Physics*; Cornell University: Ithaca, NY, 1979.
(2) (a) Han, C. C.; Bauer, B. J.; Clark, B. J.; Muroga, Y.; Okada, M.; Tran-Cong, Z.; Sanchez, I. C. *Polymer* **1988**, *29*, 2002. (b) Shibayama, M.; Yang, H.; Stein, R. S.; Han, C. C. *Macromolecules* **1985**, *18*, 2179. (c) Schwahn, D.; Mortensen, K.; Yee-Maderia, H. *Phys. Rev. Lett.* **1987**, *58*, 1544.
(3) Sakurai, S.; Jinnai, H.; Hasegawa, H.; Hashimoto, T.; Han, C. C. *Macromolecules* **1991**, *24*, 4839.
(4) Schwahn, D.; Mortensen, K.; Springer, T.; Yee-Maderia, H.; Thomas, R. *J. Chem. Phys.* **1987**, *87*, 6078.
(5) Wignall, G. D.; Bates, F. S. *J. Appl. Crystallogr.* **1987**, *20*, 28.
(6) Sakurai, S.; Hasegawa, H.; Hashimoto, T.; Hargis, I. G.; Aggarwal, S. L.; Han, C. C. *Macromolecules* **1990**, *23*, 451.
(7) Mays, J. W.; Hadjichristidis, N.; Fetters, L. J. *Macromolecules* **1985**, *18*, 2231.
(8) Brandup, J.; Immergut, E. *Polymer Handbook*, 3rd ed.; Wiley: New York, 1989.
(9) Bidkar, U. R.; Sanchez, I. C. *Macromolecules* **1995**, *28*, 3963.
(10) Dudowicz, J.; Freed, K. F. *J. Chem. Phys.* **1992**, *96*, 9147.
(11) Dudowicz, J.; Freed, K. F. *Macromolecules* **1991**, *24*, 5112.
(12) Schweizer, K. S. *Macromolecules* **1993**, *26*, 6033.
(13) Curro, J. G.; Schweizer, K. S. *Macromolecules* **1991**, *24*, 6736.
(14) Binder, K. *J. Chem. Phys.* **1983**, *79*, 6387.
(15) Khokhlov, A. R.; Erukhimovich, I. Y. *Macromolecules* **1993**, *26*, 7195.

MA951220D